

DESIGN OF THE RF SYSTEM OF RIKEN SSC

T. Fujisawa, K. Ogiwara, S. Kohara, Y. Oikawa, I. Yokoyama, M. Hara, I. Takeshita and Y. Chiba
The Institute of Physical and Chemical Research, Wako-Shi Saitama 351, Japan

1. Summary

A new movable box type variable frequency resonator is designed for the RIKEN SSC. This resonator is a compact half wave length coaxial type (2.1 m(H) × 3.5m(W) × 1.6m(D)). The delta shape dee is supported in median plane by vertical stems in opposit sides. The resonant frequency is varied from 20 to 45 MHz by moving the boxes surrounding the stems. These boxes are not in contact with the stems but with the wall of the resonator. The power losses are moderate for required dee voltages. The maximum dee voltage is 250 kV at 45 MHz. The resonant frequency, Q-value, shunt impedance and voltage distribution along the accelerating gap have been studied on a one fourth model. The power amplifier is to supply the maximum RF power of 300 kW. An RCA 4648 tetrode is to be used for the final amplifier in grounded cathode configuration. The RF power is fed into the resonator through a 50Ω coaxial feeder line (~1.5 m length) which is coupled with the resonator in good impedance matching by a variable capacitive coupler. Load resistance matching for the tube is made by a variable capacitor inserted in series at the output port of the amplifier. The final amplifier and its components are studied on a full sized model.

2. Introduction

The RIKEN separated sector cyclotron(SSC) is under construction and will be completed in 1986. The general features of the SSC are described elsewhere¹ and the present status in this conference². The basic design of the RF system was already reported³. In Table 1, the characteristics of the RF system are summarized. In advance of construction the resonator and final amplifier are studied on models in order to design in more detail, and some improvements and changes are made. The main change is that the lowest frequency of the resonator is altered from 17 MHz to 20 MHz. In this paper the current design of the RF system is described.

Table 1 Characteristics of the RF system.

Number of resonators	2
RF frequency	20 ~ 45 MHz
Harmonic NO.	5, 9, (10), (11)
RF peak voltage	250kV at 45 MHz
Frequency stability	10 ⁻⁸
Voltage stability	10 ⁻⁴
Phase stability	< 1°
Mean injection radius	89.3cm
Mean extraction radius	356cm
Dee angle	23.5°
Output power of each RF amplifier	300kW

3 Resonator

The resonator designed previously³ is a conventional coaxial type which covers a frequency range of 17 to 45 MHz by movable shorting plates. However, it has some disadvantages;

1) The height of the resonator is very high(7.5 m) and

traveling distance of the shorting plate is long (2 m). Consequently, the total height of resonator including the driving mechanism of the shorting plate becomes more than 11 m.

2) The maximum current density at the sliding contact of the shorting plate is estimated to be 70 A/cm at dee voltage (V_{dee})=250kV for 45 MHz. It is difficult to fabricate the sliding contact which endure such high current density.

Therefore, a new movable box type resonator is designed. In Fig. 1, the illustration of the resonator is shown. This resonator is a half wave length coaxial type. The RF voltage has nodes at the upper and lower ends of the resonator, and is maximum at the median plane. The resonant frequency is varied by moving the boxes surrounding the stems.

The resonant frequency of a tank circuit is given by $f = 1/2\pi\sqrt{LC}$ where L is the inductance of the circuit and C is the capacitance. If the resonant frequency of the circuit is varied from f₁ to f₂ by changing only L or C, the changing ratio of L or C must be (f₁/f₂)². In the case of the movable shorting plate type resonator, only L is varied. Then the travelling length of the shorting plate becomes very long if the resonant frequency is varied in a wide range of 20 to 45 MHz. On the other hand, in the case of the movable box type resonator both the L and C are varied by moving the boxes so the height of the resonator and travelling length of the boxes become shorter than those of the movable shorting plate type. In our preliminary calculation⁴, the height of the resonator is less than 3 m and the travelling length of the box is about 0.6 m. This resonator has another advantage that current densities at the sliding short fingers become much lower than those at the ends of the stems because the boxes are in contact with only the wall.

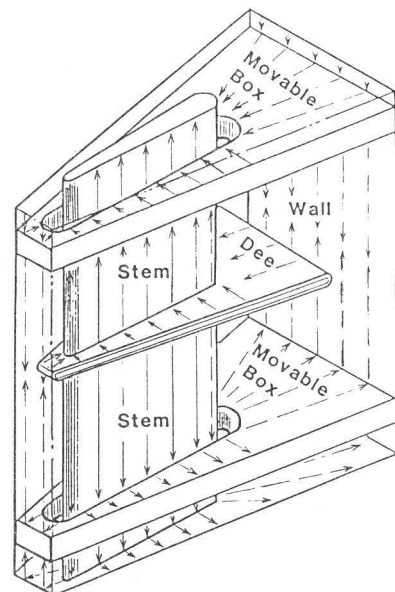


Fig.1. Illustration of a movable box type resonator. The arrow shows electric current flow.

One fourth Model Resonator

On the basis of the calculations of transmission line approximation⁴, the 1/4 scale model resonator was constructed to investigate the RF characteristics and the method of fabrication in detail. The calculation was carried out assuming that the electric currents flow as shown in Fig. 1 and their densities at the same distance from the stem ends are proportional to the capacitances in an unit area. Figure 2 shows a photograph of the 1/4 scale model resonator. Resonant frequency is changed coarsely by a pair of movable boxes and finely by a trimmer capacitor which is opposite to the dee. The RF power is fed through a coaxial feeder line of 50 ohm wave impedance. The impedance of the resonator is matched with that of the feeder by a movable capacitive coupler which is attached to the top of the feeder.

Q-values of the actual resonator are estimated by multiplying the measured Q values by the scale factor of $\sqrt{4}$ and resonant frequencies by 1/4. In Fig. 3, Q-values and resonant frequencies deduced from the

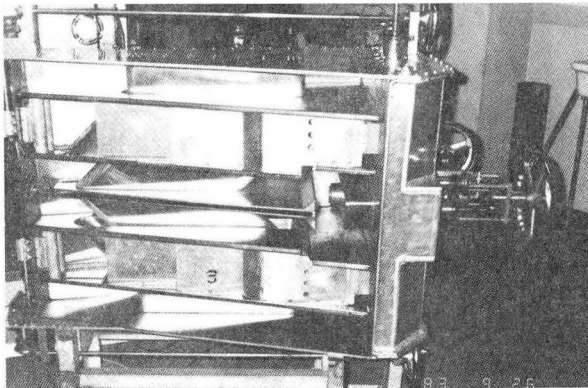


Fig.2. Picture of one fourth scale model of the movable box type resonator. The dimensions (height \times width \times depth) of the resonator are as follows (mm): Inside of the resonator; (675 \times 875 \times 440), Dee; (25 \times 675 \times 327), Stem; (325 \times 438 \times 50), Movable box; 162 h). Gap between the stem and movable box ; 10.

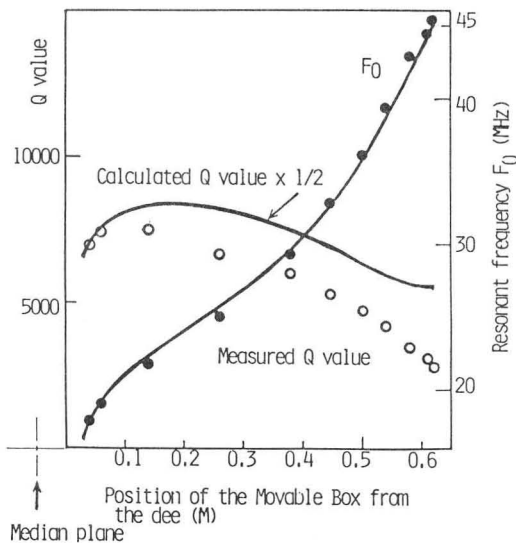


Fig.3. Q values and resonant frequency of the actual resonator estimated by the experimental results. Solid lines show the values calculated by transmission line approximation.

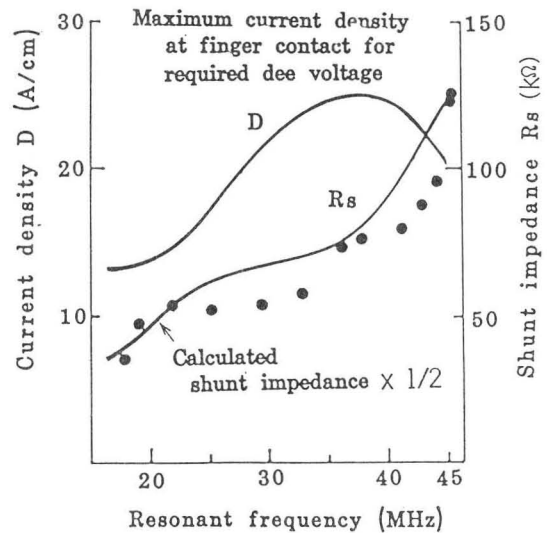


Fig.4. Shunt impedance estimated by the model test and maximum current density at finger contact estimated for the required dee voltage by the calculation.

experimental results are shown against the positions of the movable box together with the values calculated by the transmission line approximation. The resonant frequencies measured are well reproduced by the calculation. However, the measured Q-value is lower than a half of the calculated one. One reason of the poor agreement is attributed to poor contact between the movable box and the outer wall in the model. Another reason considered is that the resonator is too complex to be calculated in terms of one-dimensional transmission line. We are now trying to explain this disagreement and improve the characteristics of the model.

The shunt impedance R_s is given by $R_s = V_{dee}^2 / (2P)$, where P is the power loss of the resonator. The shunt impedance of the model is deduced from measurements of the dee voltage and RF power fed into the resonator. The shunt impedance of the actual resonator is estimated by multiplying the model's value by the scale factor of $\sqrt{4}$. In Fig. 4 the shunt impedances measured and calculated are shown against the resonant frequency. The estimated maximum current density at the sliding contact for the required dee voltage is also shown. The tendency of the calculated R_s is agreement with measured one but the absolute value is about twice of measured one. The estimated current density is within practical limit.

At a resonance point of the resonator including the coupling capacitance C_f (See Fig. 6), impedance Z_1 take a real value and its magnitude is given by $|Z_1| = 1 / (2\pi F_0 C_f)^2 R_s$. The impedance matching means that Z_1 is equal to real 50 ohms. It is realized by adjusting C_f and tuning the resonator. The matching was obtained by changing C_f from 1 pF for 45 MHz to 7pF for 17 MHz.

Relative distributions of RF electric field along the dee gap were measured by perturbation method.⁶ The results are shown in Fig. 5, where the dee voltages are normalized at beam injection radius.

Final design of the resonator

As shown in Fig. 5 the voltage at the extraction point is higher than that at injection point but the voltage distribution has the minimum at around position 5. This minimum arises from the fact that the stem is connected at large radius of the end of the resonator in order to reduce the power loss (See Fig.2). The radially increasing distribution is more desirable for good quality beam⁶. Such distributions will be

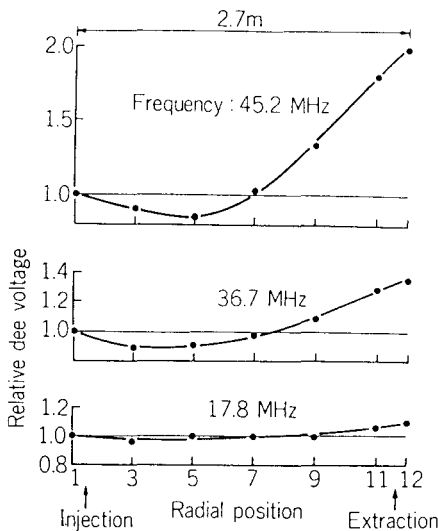


Fig.5. Relative distributions of RF electric field along the dee gap. The frequency shown is one fourth of the measured one.

obtained by a resonator whose straight stems are connected at center side edge of the dee (See Fig. 1). However, it is difficult to realize the radially increasing distribution in the frequency range of 17 to 45 MHz because in our calculation the power loss of the resonator whose straight stems are connected to the dee at 20 cm from the center side edge of dee is much higher than that of the present model. Therefore we change the lowest frequency from 17 MHz to 20 MHz and design the resonator again in order to obtain good voltage distribution. In this case the same range of energy and nuclide that is realized in the frequency range of 17 to 45 MHz is realized by changing the harmonic number from 9 to 10 or 11². The resonator designed newly and its frequency characteristics are shown in Ref. 2. The maximum input power for required dee voltage became about 200 kW. The height of resonator is 2.1 m and that of movable box 0.26 m.

4. Power Amplifier

Each of two resonators is to be powered by a separate RF amplifier capable of delivering 300 kW in a frequency range of 17 to 45 MHz⁺. A schematic diagram of the final stage of the amplifier is shown in Fig. 6. An RCA 4648 tetrode is to be used in grounded cathode configuration. Structure of the final amplifier and its RF characteristics were investigated on a full sized model^{8,9,10}. The cross sectional view of the model is shown in Ref.2.

Plate circuit

The plate circuit is tuned by a quarter wave length coaxial stub having a movable short. The stroke of the movable short is about 1.7 m to cover the frequency range. RF power is fed into the resonator through a 50 ohm coaxial feeder line (~ 1.5 m length). Load resistance matching for the tube is made by a variable capacitor C_s (20 ~ 200pF) inserted in series at the output port of the amplifier. The impedance matching condition between the tube and feeder line was

+ In the study of the amplifier system the frequency range was from 17 to 45 MHz. The resonant frequency of the new resonator reaches to 17 MHz though the power loss becomes large. Therefore the frequency range of the amplifier is not changed.

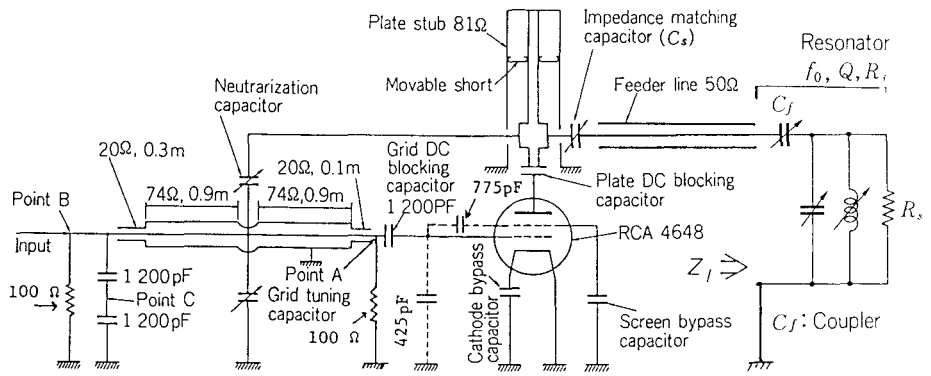


Fig.6. Schematic drawing of the final stage amplifier of the RIKEN SSC.

investigated on the model whose output port was terminated by an equivalent dummy load of 50 ohms⁸. The load impedance can be varied from 150 to 400 ohms at any frequency in the range.

The DC blocking capacitor of plate tuning circuit must sustain DC voltage of 18 kV and high RF current of 220 A(rms) at 45 MHz⁹. Large capacitance is desirable to reduce the RF voltage across the capacitor. Coaxial structure of the plate circuit suggests to use a ring array of capacitors surrounding the plate terminal. Such an array is expected to have self resonances which disturb normal circuit operation. We made an array using four commercially available 400 PF ceramic capacitors (Toshiba RDF110CS) whose terminal block was made shorter and its diameter larger in order to reduce the inductance. The self resonances were found at around 50 and 70 MHz. They are half wave length and full wave length resonances on the array, respectively. The reactive power rating of the blocking capacitor is required to be more than 120 KVA at 45 MHz. We are trying to get at least the power rating of 120 kVA at 45 MHz by cooling the improved terminal of the capacitor by water.

Screen grid bypass capacitor

In Fig. 7(a), the simplified circuit diagram of the final amplifier is shown. The symbols $C_0 \sim C_4$ show the interelectrode capacitances and C_5 shows the capacitance of the screen bypass. For the stable operation of the amplifier, it is necessary to reduce the coupling between the plate and control grid to a value as small as possible. A part of the coupling is due to the direct interelectrode capacitance C_0 . The other part is attributed to the screen bypass C_5 which takes a finite value. The latter effect can be replaced equivalently by an additional capacitance C^* to C_0 as shown in Fig. 7(b). For the stability of the amplifier, it is important to use a screen bypass capacitor which gives sufficiently low impedance without resonances in a wide frequency range. The screen bypass capacitor was made in order to study the performance^{2,11}. The both sides of the screen contact plate (450 mm(W) × 600 mm(D)) are insulated by (50 μm) kapton films from the upper and lower ground surfaces and forms the capacitor of 0.11 μF. The 50 μm kapton film could endure a voltage as high as 5 kV DC for a long time in a preliminary test.

The capacitor was mounted on the model amplifier and the voltage transmission ratio from the plate to the screen and control grids were measured. The flat frequency responses are obtained in a frequency range of 1 to 100 MHz¹¹. This fact shows that this capacitor operates well in this frequency range. The capacitance C_0 deduced from the ratio is 1.5 pF. The value of C^* for $C_5 = 0.11 \mu F$ is 0.5pF. The measured value of C_0 is 2.5 times the value given in the catalogue. In Fig. 7,

Capacitances in the catalogue (measured)

- | | |
|----------------------------------|----------------------|
| $C_0 = 0.6 \mu\text{F}$ (1.5 pF) | P: Plate |
| $C_2 = 85 \text{ pF}$ (=75 pF) | G_1 : Control grid |
| $C_3 = 775 \text{ pF}$ (737 pF) | G_2 : Screen grid |
| $C_4 = 425 \text{ pF}$ (357 pF) | K: Cathode |
| $C_1 = 4.5 \text{ pF}$ | |

$$C^* = (C_2 \cdot C_3) / C_5 \text{ for } (C_2, C_3 \ll C_5)$$

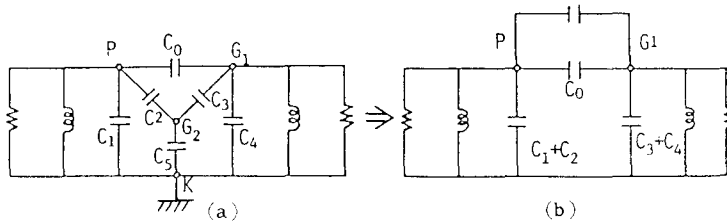


Fig.7. (a) Simplified diagram of the 4648 and amplifier.
(b) Equivalent circuit for (a).

the interelectrode capacitances measured are shown. They are a little different from those in the catalogue. The capacitance C^* for $C_5 = 0.11 \mu\text{F}$ is one third of C_0 . In stability consideration of the amplifier it is indispensable to take account of the coupling effect of this order of magnitude. This capacitance has been used for RILAC amplifier and been working well for about two years.

Grid Tuning Circuit

The necessary grid RF driving voltage is estimated to be 300 V to deliver output power of 300 kW. For driving the large input capacitance of the 4648, nominal 1200 pF, it is attractive to use the same broad band bridged-Tee network that has been working well in lower frequency region below 25 MHz¹³. In our case, however, this circuit is not practical because this network needs remarkably higher driving power as the operating frequency becomes higher. Furthermore, the voltage node is at 2 cm outside from the grid terminal at 45 MHz. Therefore, a full wave length coaxial type tuning circuit having a tuning capacitor at the median of the line is designed. A basic design of the circuit has previously been reported^{3,12}. Subsequently it was noticed by experience on the amplifier of RILAC¹¹ that a lower shunt impedance of the grid circuit is vital for the stable operation and neutralization is effective in high frequency range. Therefore, we took following two modifications:¹⁰

- 1) The shunt impedance at the grid is reduced to 12.5 ohm while the input impedance is kept at 50 ohm;
- 2) A small variable capacitor between the plate and the tuning capacitor is added for neutralization.

The performance of the improved circuit was studied on a full sized model equipped with a real tube in cold state². Tuning and impedance matching are simultaneously done by adjusting the tuning capacitor. Fig. 8 shows the results of measurement for tuning characteristic and input impedance of the grid circuit against the frequency. The intended performance is obtained in a frequency range of 17 to 45 MHz. The effect of the neutralization was studied at 40 MHz by measuring the voltage transmission ratios from the plate to points A and B in Fig. 6. The voltages induced at points A and B are reduced to one fifth of the voltage without the neutralization.

5. Conclusions

In this report the DC power supply for the amplifier and the stabilizer systems of the dee

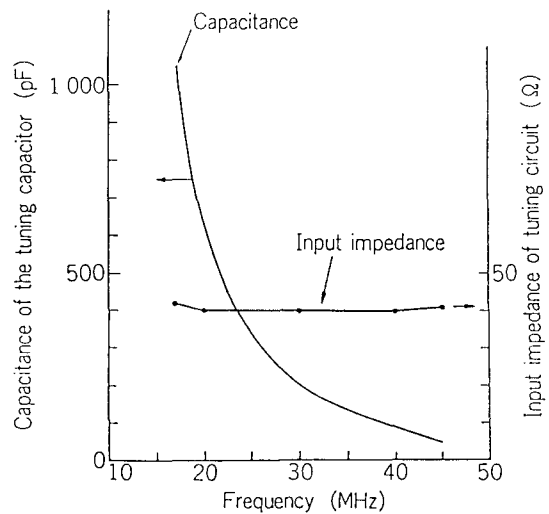


Fig.8. Capacitance of the tuning capacitor and input impedance of the grid tuning circuit against the resonant frequency.

voltage, its phase and resonant frequency of the resonator are not represented. We are designing them referring to the amplifier system of RILAC¹⁴. The design studies on the RF system of the RIKEN SSC have made large advance. The result of the studies are promising.

References

1. H. Kamitsubo, Proc. of 9th Int. Conf. on Cycl. and their appl., Caen (1982) 13.
2. H. Kamitsubo, 'The RIKEN Linear Accelerator -Cyclotron System', This Conference.
3. M. Hara, T. Fujisawa and K. Ogiwara, Proc. of 9th Int. Conf. on Cycl. and their appl., Caen (1982) 411.
4. T. Fujisawa, RIKEN Accel. Prog. Rep., NO 15 (1981) 196, K. Ogiwara, T. Fujisawa and Y. Oikawa, ibid NO 16 (1982) 217.
5. K. Ogiwara, T. Fujisawa and Y. Oikawa, 'Model study of the RF resonator for RIKEN SSC' ibid NO 17 (1983).
6. L. C. Maier, Jr and J. C. Slater, J. Appl. Phys. 23 (1952) 68.
7. A. Goto, N. Nakanishi and Y. Yano, 'Computer Simulations of accelerated Particles in the RIKEN SSC', This Conference.
8. T. Fujisawa, S. Kohara, K. Ogiwara, Y. Oikawa and Y. Kumata, 'Study of the RF power amplifier for the RIKEN SSC' ibid NO 17 (1983).
9. S. Kohara, T. Fujisawa, and Y. Chiba, 'Study of the plate DC blocking capacitor', ibid NO 17 (1983).
10. T. Fujisawa, S. Kohara, K. Ogiwara, Y. Oikawa and Y. Kumata, 'Grid tuning circuit of the RF power amplifier of the RIKEN SSC' ibid NO 17 (1983).
11. T. Fujisawa and Y. Chiba: RIKEN Accel. Prog. Rep. 16 169(1982), S. Kohara, T. Fujisawa and Y. Chiba: ibid 171, S. Kohara and T. Fujisawa: ibid 175.
12. S. Kohara and T. Fujisawa; RIKEN Accel. Prog. Rep. 16 173(1982).
13. S. W. Mosko, J. D. Raylander, G. K. Schulze: IEEE Transactions on Nuclear Science, Vol. NS-24, NO 3, June, 1786(1977).
14. Y. Chiba, IPCR Cycl. Prog. Rep. NO14(1980) 120, ibid NO 13(1979) 143.